Large-Scale Activity in the Bastille Day 2000 Solar Event

I.M. Chertok
IZMIRAN, Troitsk, Moscow Region, 142190 Russia

V.V. Grechnev
Institute of Solar-Terrestrial Physics, P.O. Box 4026, Lermontov Street 126, Irkutsk 664033, Russia

Abstract.

We have analyzed dimmings (i.e. transient coronal holes) and manifestations of a coronal wave in the famous event of 14 July 2000 using images produced with the EUV telescope SOHO/EIT. Our analysis was inspired by a paper of Andrews (2001), in which this event was studied using *running*-difference EIT images at 195 Å formed by the subtraction of a previous image from each current. *Running*-difference images emphasize changes of the brightness, location, and configuration of observed structures occurred during the 12-min interval between two subsequent heliograms. However, they distort the picture of large-scale disturbances caused by a CME, particularly, dimmings. A real picture of dimmings can be obtained when derotated *fixed*-difference images are considered. The latter are formed in two stages: first, the solar rotation is compensated using three-dimensional rotation of all images ('derotation') to the time of a pre-event heliogram, here 10:00 UT, and then the base heliogram is subtracted from all others. We show real dimmings to be essentially different from those described by Andrews (2001). The reconstruction of large-scale magnetic fields in the corona in connection with the CME is accompanied by the appearance and growth of two large dimmings. One of them is located along the central meridian, southward of the eruptive center, at the place of the pre-eruptive arcade. Another dimming occupies the space between the flare region and a remote western active region. Moreover, fragmented dimmings are observed virtually overall on the solar disk, especially, within the northwest quadrant. A propagating disturbance with properties of a coronal wave has been also revealed in the north polar sector. We also suppress the 'snowstorm' produced in the EIT images by energetic particles that allows us to consider the dimming manifestations in all four passbands 171, 195, 284, and 304 Å, as well as the light curves of the main dimmings including several later images at 195 Å.

1. Introduction

The 'Bastille Day Event' occurred on 14 July 2000 at about 10:20 UT in the central active region AR 9077 (N22 W07) and around it. This famous event was one of the largest solar eruptive events in the 23$^{\rm rd}$ cycle and included a filament eruption, long-duration 3B/X5.7 flare, and rapid halo-type coronal mass ejection (CME). It was accompanied particularly by a strong flux increase of solar energetic particles in the

interplanetary space ($J_{>10\,\mathrm{MeV}} \sim 10^4\,\mathrm{cm}^{-2}\,\mathrm{sr}^{-1}\,\mathrm{s}^{-1}$) and by a severe geomagnetic storm ($D_{\mathrm{st}} \sim -300\,\mathrm{nT}$).

Various features of the event were observed and studied based on the data gathered with the imaging X-ray, EUV, white-light telescopes aboard the spaceborne observatories *Yohkoh* (Ogawara *et al.*, 1991), Solar and Heliospheric Observatory (SOHO; Domingo *et al.*, 1995), and Transition Region and Coronal Explorer (TRACE; Handy *et al.*, 1999) as well as with a number of ground-based instruments of different ranges. The results of those studies were published in the special volume of *Solar Physics*, v. 204, Issue 1-2, 2001, and elsewhere.

In particular, according to Deng *et al.* (2001) and Tian, Wang, and Wu (2002), the evolution of the magnetic nonpotentiality is responsible for the energy build-up over the active region and beneath the eruptive filament. Yan *et al.* (2001) carried out the force-free reconstruction of the three-dimensional magnetic field structure and compared it with observed EUV loops during the flare maximum. Kosovichev and Zharkova (2001) detected large-area variations of the magnetic field in the lower solar atmosphere during the flare. Fletcher and Hudson (2001) studied the generation of EUV flare ribbons and showed their relation to the magnetic structure and reconnection. In this flare, a clear hard X-ray (HXR) two-ribbon structure was observed for the first time with the *Yohkoh* HXR telescope (HXT) in the energy range 30–90 keV (Masuda, Kosugi, and Hudson, 2001). At the post-eruption stage of the event, the Yohkoh soft X-ray telescope (SXT) and the EUV telescopes aboard SOHO and TRACE recorded the development of a huge arcade, with a width of $\sim 30\,000$ km and a length of $\sim 120\,000$ km, that consisted of numerous emitting loops brighteninig up in a sequential manner from highly-sheared low-lying to less-sheared higher-lying bipolar loops (e.g., Achwanden and Alexander, 2001). Somov et al. (2002) argued that the structure and dynamics of the HXR flare kernels and ribbons can be explained in terms of the three-dimensional reconnection at a separator in the corona described by so-called 'rainbow reconnection' model.

A number of studies (e.g., Caroubalos *et al.*, 2001; Chertok *et al.*, 2001; Karlický *et al.*, 2001; Klein *et al.*, 2001; Maia *et al.*, 2001; Reiner *et al.*, 2001) dealt with the wide-range radio emission associated with the flare, CME, CME-driven shock, and the posteruptive energy release. In the given event, γ-ray emission with a photon energy up to ~ 10 MeV was observed on *Yohkoh* during 20 min (Share *et al.*, 2001). The time and place of the particle acceleration responsible for the solar emission in different ranges and the relativistic proton enhancement detected at 1 AU were discussed particularly by Klein *et al.* (2001) and Livshits and Belov (2004).

The present study was motivated by a paper of Andrews (2001) (hereafter referred to as Paper 1) considering observations of the coronal activity with two SOHO instruments: the Large Angle Spectroscopic Coronagraph (LASCO; Brueckner *et al.*, 1995) and the Extreme ultraviolet Imaging Telescope (EIT; Delaboudinière *et al.*, 1995). LASCO provided detailed data on CMEs associated with the Bastille Day event and two other preceding X-class flares from the same active region on 11 and 12 July. In particular, for the Bastille Day event, the sky-plane component of the initial speed of several features on the leading edge of the halo CME at the heliocentric distance of $2R_\odot$ was derived to range from 1700 to 1300 $\mathrm{km\,s^{-1}}$ with a clear deceleration from -40 to $-120\,\mathrm{m\,s^{-2}}$. However, the description and analysis of the flare brightening and CME-initiated dimmings visible on the EIT heliograms presented in Paper 1 contain essential inaccuracies.

Let us remind that dimmings (i.e. transient coronal holes) appear after big CMEs as large-scale areas and structures of a reduced brightness of the EUV and soft X-ray emission persisting for many hours (e.g., Thompson *et al.*, 1998; Zarro *et al.*, 1999; Gopalswamy and Thompson, 2000; Webb, 2000; Hudson and Cliver, 2001). The dimmings in the Bastille Day event are studied using 12-min sequence of SOHO/EIT fulldisk 195 Å images sensitive to the coronal plasma at a temperature of $\sim 1.5 \times 10^6$ K. In the text and caption to Figure 2 of Paper 1, the author writes that each of the considered images is the difference of the heliogram at the indicated time and the same frame prior to the event at 10:00 UT (we shall call such images *fixed* or *base* difference images). However, the images shown in Figure 2 and described in the text of Paper 1 are in the reality *running*-difference images formed by successive subtraction of each preceding frame from each current one. Some EIT running-difference images of the Bastille Day event were also considered by Klein *et al.* (2001). Meanwhile it is clear (see the next Section) that just fixed-difference images, but not running ones, display the true picture of the flare and CME disturbances as well as their real evolution. An additional important point is that the formation of such images requires a prior compensation of the solar rotation, i.e. 'derotation' of the heliograms. That is why in the present paper, we analyze the Bastille Day event based on the EIT derotated fixed-difference images at 195 Å. We also suppressed the 'snowstorm' produced by energetic particles that strongly affects late images of the Bastille Day event. This allowed us to consider the dimming manifestations in a special type of derotated difference images with a 6-hour interval in all four EIT passbands 171, 195, 284, and 304 Å.

The method to study dimmings which we use is outlined in Section 2. By means of this method we analyze SOHO/EIT images observed in the

course of the Bastille Day event in Section 3. We discuss and summarize the results in Section 4.

2. Method

The method is based on the analysis of 'derotated' *fixed-difference* images and involves the following items: (1) preparation of the images, (2) compensation for the solar rotation in the images ('derotation'), (3) subtracting the images, (4) suppression of the 'snowstorm' produced by energetic particles, (5) appropriate nonlinear representation of the images to reveal large-scale activity manifestations, and (6) quantitative analysis.

First, we process all SOHO/EIT images using the IDL[1] routine EIT_PREP.PRO. This routine performs background subtraction, degridding images, and a flat-field correction. Next, the images are properly oriented, centered, and variations of the exposure time are corrected. We also resize all the images to 512×512 pixels, which is sufficient to study such large-scale features as dimmings, but reduces the time consumation in data processing.

There is an essential distinction between fixed and running difference representations. The latter, being, in fact, an approximation of the temporal derivative of the image series, emphasizes changes (of the brightness, location, and structure of features) that occurred during the time interval between adjacent frames. However, we should be aware of properties of the derivative which are manifest as artifacts inevitably appearing in the running-difference images. Any decrease of the intensity of bright features or their displacement between two adjacent frames would result in the appearance of artifactitious 'dimmings'.

In contrast, fixed-difference images show real changes that occur during the events relative to the selected reference frame before the event. Nevertheless, another problem arises here because some false features can also appear due to the solar rotation. In the 512×512 pixel EIT images with a pixel size of $5''.24$, the rotation effect appears to be almost inessential when difference images (as running ones) are obtained by subtracting heliograms taken 12 min apart. However, the solar rotation becomes important if the interval between frames exceeds tens of minutes, as in the case of the fixed-difference images. In particular, the displacement of any feature due to the solar rotation results in the appearance of the false eastern edge of the opposite contrast in the difference image. This effect is most pronounced for narrow

[1] IDL is the trademark of the *Research Systems, Inc.*

features disposed nearly along the meridian, e.g., filaments going in NS directions and transequatorial loops, where the longitudinal extent of the artifactitious edge is comparable with the size of the feature itself.

To avoid the appearance of false darkenings and brighenings, before the formation of the difference images, we compensate the rotation of the Sun by means of the 'derotation' of all heliograms to the same selected time, usually to the time of the reference frame before the event. In the software used, the solid rotation is applied to the whole visible solar hemisphere, and the spherical surface at the photospheric radius is rotated. Such a variant of the derotation is not perfect particularly because in the reality, the solar rotation is not solid, and 3D structures observed in the EUV range comprise some altitude interval at larger heliocentric distances. However, possible errors due to the solid rotation of the sphere at $1R_{\odot}$ are small and cannot change noticeably the observed picture of the dimmings and other features, especially for events occurring in the central sector of the solar disk.

To 'rotate' a solar image around the solar polar axis, we first convert the rectangular sky-plane coordinates of pixels on the visible solar surface into the longitude and latitude. Then we transform the longitudes according to the solar rotation during the required time interval, and convert the longitudes and latitudes to the sky-plane coordinates again. Finally, we transform the solar image to the last coordinates. The coordinate-conversion IDL routines were developed by M. J. Aschwanden.

In our previous papers, we used the SOHO/EIT derotated fixed-difference images to study anisotropic large-scale channeled dimmings typical for the complex global solar magnetosphere near the cycle maximum (Chertok and Grechnev, 2002, 2003a) and to analyze the dimmings simultaneously in four multi-temperature lines by the heliograms recorded with 6- and 12-hour intervals (Chertok and Grechnev, 2003b,c). The outlined technique has also been applied to demonstrate the homology of large-scale EUV disturbances (dimmings and coronal waves) associated with the 24–26 November 2000 series of six recurrent major flares and halo CMEs (Chertok *et al.*, 2004a) as well as to study the post-eruptive activity following one of the most powerful eruptive event of 4 November 2001 by data of the SPIRIT telescope (Zhitnik *et al.*, 2002) aboard the CORONAS-F spacecraft (Oraevsky and Sobelman, 2002; Oraevsky *et al.*, 2003) in three EUV channels (Chertok *et al.*, 2004b).

In the present paper, we analyze the Bastille Day event based on the EIT derotated fixed-difference images in the 195 Å coronal line.

In contrast to Paper 1, the running-difference images are used as an auxiliary tool and are shown for the comparison only.

An additional methodical point in the study of the Bastille Day event is concerned with a 'snowstorm' produced by solar energetic particles (SEP) arriving to the telescope from this flare. Starting with 11:00 UT, the EIT heliograms are covered more and more by numerous bright points and streaks caused by the increasing SEP flux. To suppress this effect, we use two techniques. The essence of the first way is 1) to find 'snowflakes' in a current image as drastic brightenings with respect to the preceding image, and then 2) to replace each pixel within 'snowflakes' with its minimum value from adjacent images. This way allows us considering several 195 Å heliograms after 11:00 UT. Possible artifacts introduced by this image processing are limited within three consecutive frames, or ±12 minutes.

The second way is to form difference images displaying only darkening regions, particularly dimmings. It is useful if one pre-event and one post-event images are only available. In this way, to each pixel of the image from which the base frame is subtracted, we assign its minimum value of both these images. The second way enables to use the 13 UT heliograms at 171, 195, 284, and 304 Å and to visualize dimmings in the derotated difference images with 6-hour interval simultaneously in all four EIT diverse-temperature lines. As can be expected, the visibility of dimmings in such images strongly depends on the exposure time with which the heliogram was observed.

Dimmings are relatively faint features with respect to flares simultaneously observed, and usually do not exceed few percent of the maximum brightness in a frame. Hence, to show them clearly, we restrict the brightness in the difference images. It is important to show the negative pixel values, because the brightness in dimming regions decreases with respect to the initial frame. Therefore, we use symmetric positive and negative thresholds.

To study the dimmings quantitatively, we compute time profiles in a few small regions on the solar disk in the same way as Zarro *et al.* (1999) did. These light curves allow estimating the depth of the dimming and show the evolution of its various parts as well as their temporal relation.

Both fixed and running images at 195 Å as well as the corresponding movies and other relevant illustrations are presented at the web site http://helios.izmiran.troitsk.ru/lars/Chertok/000714n/index.html.

3. Analysis of the SOHO/EIT images

3.1. Fixed-difference images

Before and during the Bastille Day event, EIT recorded full-disk images at 195 Å with 12-min time intervals. A noticeable activity, mainly such as relatively small-scale brightenings and darkenings, occurred almost continuously inside and nearby AR 9077 before 10:00 UT. However, the first essential flare brightening is displayed by the 10:12 UT image. Therefore, following Paper 1, we take the 10:00 UT heliogram as a pre-event reference image. From the movies presented at the Web site mentioned above, one can see that the general picture of the main powerful flare- and CME-associated disturbances does not change significantly if we select an earlier heliogram (for example, at 09:24 UT) as a reference image.

The situation before the event as recorded by EIT at 195 Å can be seen in Figure 1(a) where the pre-event image at 10:00 UT is presented. At least two large-scale emitting loop systems are observed southward of the elongated AR 9077 (region 1). One of them has a bright west half (1–2) perhaps related to a southeast filament channel displayed by Hα heliograms. Another loop system seems to visualize the magnetic connection between AR 9077 and a westward active region 3. An additional bright branch 1–4 originates from AR 9077 in the northwest direction.

Shown in Figure 1(b–f) are the 195 Å EIT fixed-difference images relative to the pre-event reference heliogram at 10:00 UT. The first image at 10:12 UT (b) reveals an initial flare brightening in the central part of region 1 accompanied by a weak intensification of the loops southward of it. At the same time, several relatively small-area dimmings appear around the flare brightening. The most pronounced dimming 5 together with some emitting loop-like structures is visible at the west sector of region 1 where the filament was ejected from (Klein *et al.*, 2001). The remote fragmentary darkenings, scattered throughout the disk, are identified with several active regions present on the disk, but their relation to the eruptive event is not so evident at this time. Only an east darkening 6 is connected with region 1 by a faint dimming chain.

The flare brightening culminates at 10:24 UT (c). This brightening is so strong that many image pixels are saturated, and bright artifactitious horizontal streaks have been produced together with a broad diffuse emission. Nevertheless, these do not prevent seeing the further development of the west (5) and east (7) dimmings joining to the eruptive center. Klein *et al.* (2001) classify the northwest dark fragment 8 as a manifestation of the filament ejected.

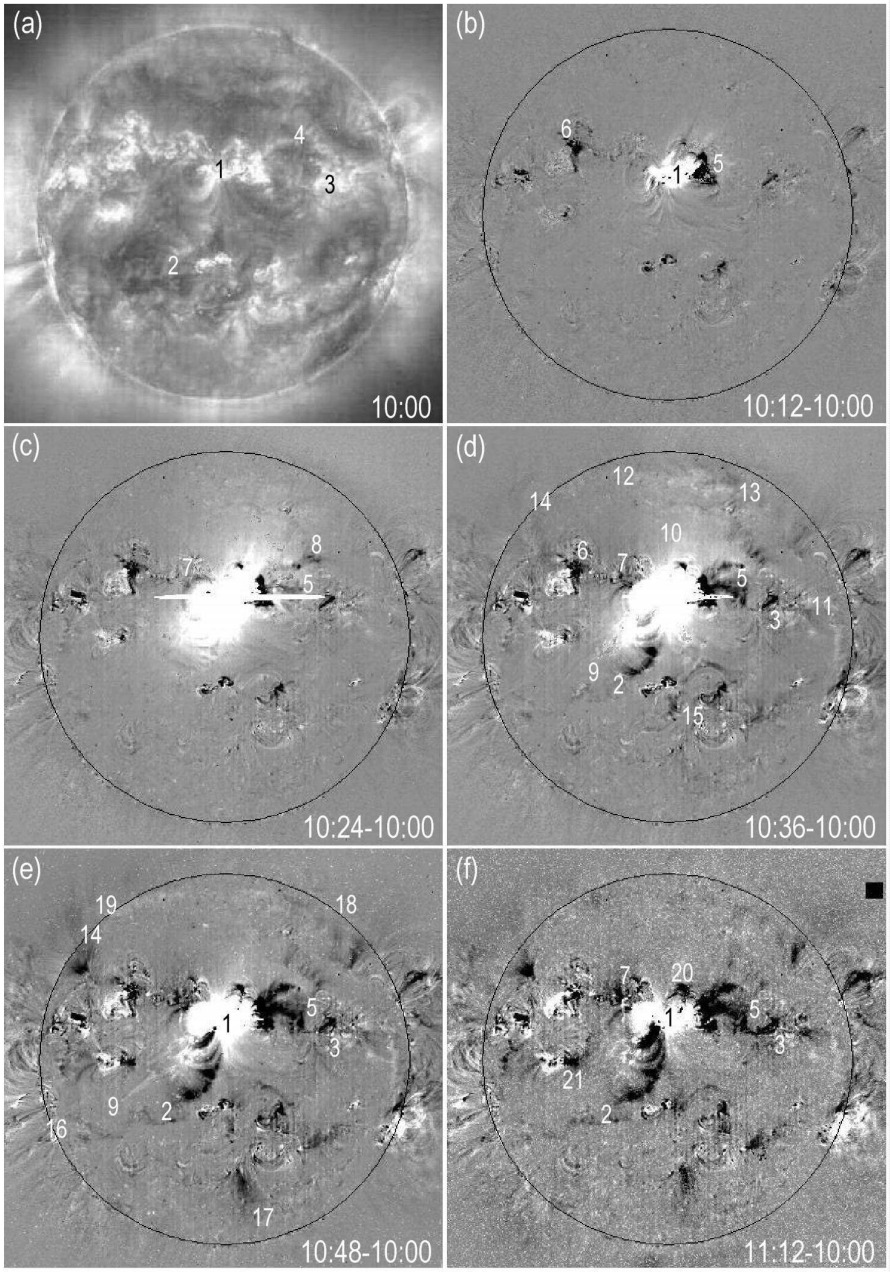

Figure 1. SOHO/EIT derotated fixed-difference images of the 14 July 2000 event at 195 Å showing CME-associated dimmings (dark regions) and saturated flare brightening relative to the reference heliogram at 10:00 UT. The 'snowstorm' from energetic particles is suppressed in frame (f).

The next fixed-difference image (d) at 10:36 UT contains remnants of the saturation but nevertheless reveals some important features of the event. The main flare brightening comprises the east (trailing) part of the active region, and a bright narrow jet 9 originates from its southeast edge. The west dimming 5 increases its area noticeably and approaches active region 3. Significant disturbances cover the whole space between the eruptive center, dimming 5, and the northwest limb. They include different dimming fragments and several curved emitting structures such as 10–11 and 12–13. It is difficult to conclude unambiguously whether these emitting structures are manifestations of a coronal wave, although some coronal wave signatures can be seen with the corresponding movie in the northwest quadrant. It seems that the emitting structure 12–13 can be identified as a coronal wave front. In the east direction, dimming 7 shows closer connection with the darkening in region 6. The latter shows a dimming continuation to the northeast limb particularly via branch 6–14. A new clear transequatorial *J*-like dimming 2 appears at the place of the brightest west element of the south pre-event arcade visible in frame (a). Some additional dimmings appear around a south complex 15, perhaps in association with the *J*-like dimming 1–2. At last, two small-area dimmings are present inside the north and south parts of the main flare brightening.

In the next frame of 10:48 UT (e), the predomination and structure of two main dimmings 1–2 and 1–5 become more and more evident. Each of them flows together with the corresponding smaller dimmings surrounding the eruptive center. The south *J*-like dimming 1–2 is observed in conjunction with several emitting loops which increased their brightness as a result of the flare. Some additional, relatively faint, narrow dimming fragments manifest themselves between the south dimming 2 and the southeast limb (16). The further advancement of the southeast jet 9 also occurs in this region. A new dimming blob 17 appears in the south high-latitude region. The west dimming 1–5 consists of a basis and two branches. The northwest branch demonstrates a conspicuous enlargement in comparison with the previous image. The west branch gets into direct touch with the remote region 3 by means of a narrow dimming channel. At least three or four quasi-radial dimming structures stretch from dimming 5 to the northeast limb (18). The probable coronal wave front 12–13, visible in frame (d), moves slightly northward and reveals evident displacement in the east direction to the northeast limb (19). Some darkening of the northeast near-the-limb dimming 14 takes place as well.

The 11:12 UT frame (f) illustrates the advanced phase of the CME-associated disturbances against the background of the enhancing 'snowstorm' from energetic particles. It should be noted that the visibility of

these disturbances is improved significantly due to the first technique of the 'snowstorm' suppression outlined in Section 2. One can see here that the flare brightening gradually decreases its extent to the sizes of the spectacular posteruptive arcade visible in original (nondifference) EIT and TRACE images (e.g., Aschwanden and Alexander, 2001). As for dimmings, all the tendencies described in the preceding paragraph are going on. In particular, two main dimmings 1–2 and 1–5–3 keep their structures, but increase their extent and perhaps darkness. As new features, one can note enlargement of the north dimming 20 and appearance of the dimming channel 7–21 between dimming blobs at the northeast edge of the posteruptive arcade and an east active region. At the same time, the northeast near-the-limb emitting fragment 19 of the assumed coronal wave cannot be further distinguished.

As the subsequent fixed-difference images show, the general picture of the CME-associated disturbances described above, particularly the south (1–2) and west (1–5) main dimmings, was observed during several hours, at least till 13 UT (see subsection 3.3).

3.2. Running-difference images

Let us consider for comparison the running-difference images presented in Figure 2. This Figure is an equivalent of Figure 2 in Paper 1, but differs from the latter by cleaner presentation of the images. It is clear that the running-difference image between 10:12 and 10:00 UT is the same as the first fixed-difference frame shown in Figure 1(b). Moreover, the next running image (a) between 10:24 and 10:12 UT has few distinctions from the second fixed frame (Figure 1c), because both these pictures belong almost to the flare maximum and are mainly formed by the strong flare brightening, its saturation, artifactitious horizontal streaks, and initial dimmings. Therefore, it is reasonable to start our consideration with the next running-difference frame (Figure 2b) keeping in mind the fixed-difference images and their description given in subsection 3.1.

A bright east feature in this frame (b) reflects real eastward displacement of the flare brightening and movement of the southeast jet 9 occurred between 10:36 and 10:24 UT. The dark features correspond mainly to two processes: the intensity decrease in the central part of the flare brightening (as well as the artifactitious horizontal streaks) and real formation of the south (2) and west (5) dimmings. In the north polar sector one can see the emitting (maybe coronal wave) front 12–13 preceded by some fragmentary darkenings.

The next running-difference image (c) between 10:48–10:36 UT is especially demonstrative. In Paper 1, it is correctly noted that in this

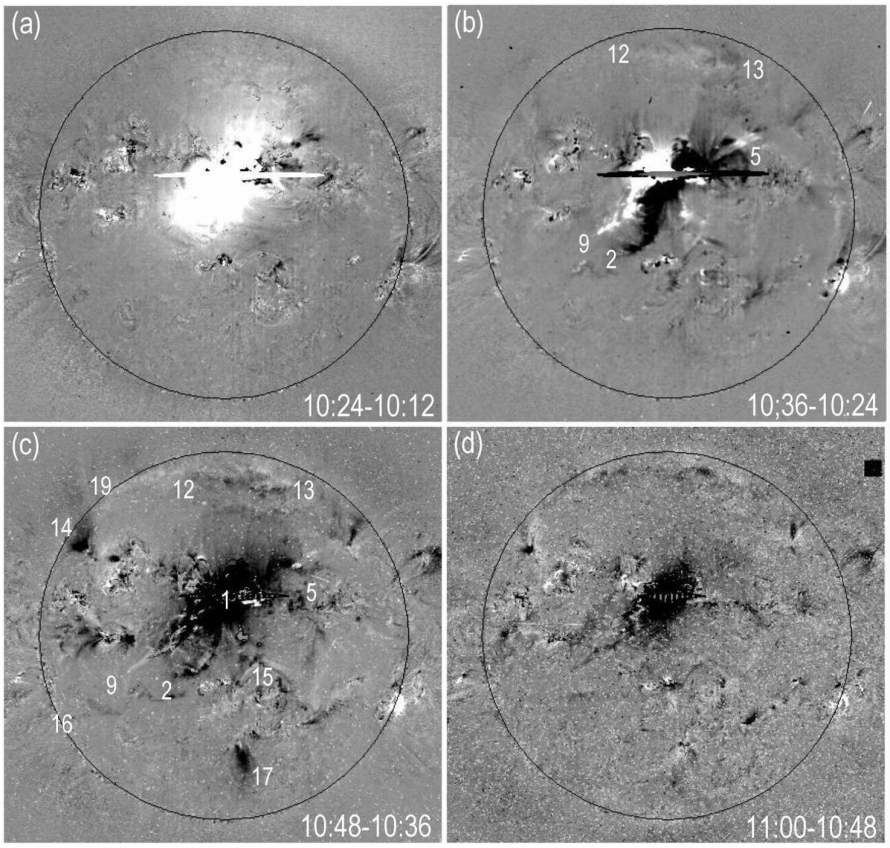

Figure 2. CME- and flare-associated disturbances of the 14 July 2000 event as visible in the SOHO/EIT running-difference images at 195 Å. The 'snowstorm' from energetic particles is suppressed in frame (d).

frame a large dark region roughly corresponds to the area that was bright at 10:24 UT (frame a). However, the conclusion of Paper 1 that this dark region is a real dimming, is erroneous. As a matter of fact, the greater central part of this darkening arises in the running-difference image (c) as a result of further intensity decrease of the flare brightening happened between 10:48 and 10:36 UT, and therefore represents a false dimming. At the same time, on the periphery of this area, some real dimmings (such as 1–2, 1–5) are also observed due to further fall of the emission intensity inside these structures, i.e., due to the increase of the dimming depth. Some remote dark elements, stretching particularly to the south region 15 and to the southeast limb 16, as well as dark blobs 14, 17, correspond to newly originated real dimmings. In direction 1–9, the dark element nearer to the eruptive center and more remote light spike show, respectively, location of the southeast jet in the previous

frame (b) and its travel to the moment of frame (c). The dark north feature 12–13 represents the site that the emitting front occupied in the previous frame, while the bright element 13–19 reveals northward and eastward displacements of this front.

At last, the running-difference frame (d) displays mainly a dark area in the center of the active region. It means that between 11:00 and 10:48 UT, on the one hand, the intensity of this part of the flare brightening continues to fall, and, on the other hand, the level of emission from the main dimming regions does not significantly change. Small bright blobs on the west and east borders of the central dark region correspond to a gradual enlargement of the longitudinal extension of the posteruptive arcade.

3.3. Four-line difference images

Due to the derotation technique, we can form the EIT difference images not only in the 195 Å line, but also at the 171, 284, 304 Å passbands using available heliograms at near 07 and after 13 UT. However, the 13 UT heliograms are covered by a strong 'snowstorm' from energetic particles. Under these conditions, to distinguish dimmings, it is reasonable to use the second way of the 'snowstorm' suppression and to produce difference images in which only structures with negative values of the resulting intensity are displayed. Such images are shown in Figure 3 for all four multi-temperature EIT passbands, including the 195 Å line. Considering these images, one should take into account that the heliograms at the indicated passbands were observed with highly different exposure times: 7.5, 12.5, 32.5, and 122.6 s at 171, 195, 304, and 284 Å, respectively. Meanwhile, it is clear that under approximately the same proton flux, the larger exposure is, the number of 'snowflakes' increases, and the visibility of the dimmings becomes worse.

One can see from Figure 3(c) that the 195 Å derotated difference image with a 6.5-hour interval reproduces the main dimmings displayed by the fixed-difference heliograms in Figure 1. We mean particularly the south J-like dimming 1–2 with its deep blob near the eruptive center, as well as the west dimming 5–3 with its multi-component basis and a narrow dimming channel going to the remote west region. Some east dimming blobs (such as 7, 14, and 21) also remain during several hours at this coronal line sensitive to the plasma temperature $T_e \sim 1.5{\times}10^6$ K.

Very similar dimmings are visible in another coronal line 171 Å with $T_e \sim 1.2 \times 10^6$ K (Figure 3b). In addition, this image reveals that the south dimming 1–2 consists of at least three semi-loops and shows many dimming blobs between the eruptive center and east limb.

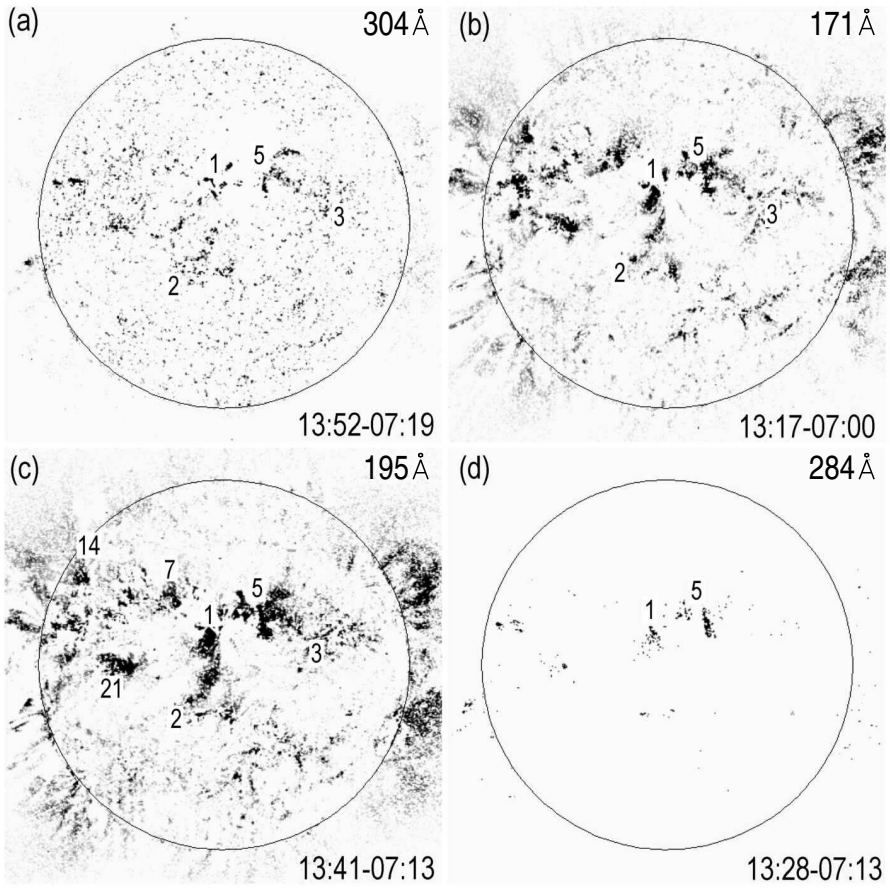

Figure 3. SOHO/EIT derotated 6-hour difference images of the 14 July 2000 event in four diverse-temperature lines 171, 195, 284, and 304 Å. For each line, the 13 UT heliogram is subjected to the suppression of the 'snowstorm' produced by energetic particles, and only dimmings (i.e. structures of negative resulting intensity) are shown. Different appearance of the images is due to different exposure times.

In the high-temperature coronal line 284 Å with $T_e \sim 2 \times 10^6$ K, the corresponding difference image (d) is very meagre. It only displays some elements of the south (1) and west (5) dimmings adjoining to the eruptive center. There are almost no other details in this image. We suppose that such a featureless character of the 284 Å image is a consequence of the very long exposure and the corresponding accumulation of a large quantity of 'snowflakes' in the 13:28 UT heliogram.

The difference image (d) in the transition-region line 304 Å with $T_e \sim (0.2-0.8) \times 10^6$ K and a moderate exposure is more interesting. It displays faint but clear fragmentary dimming structures whose location

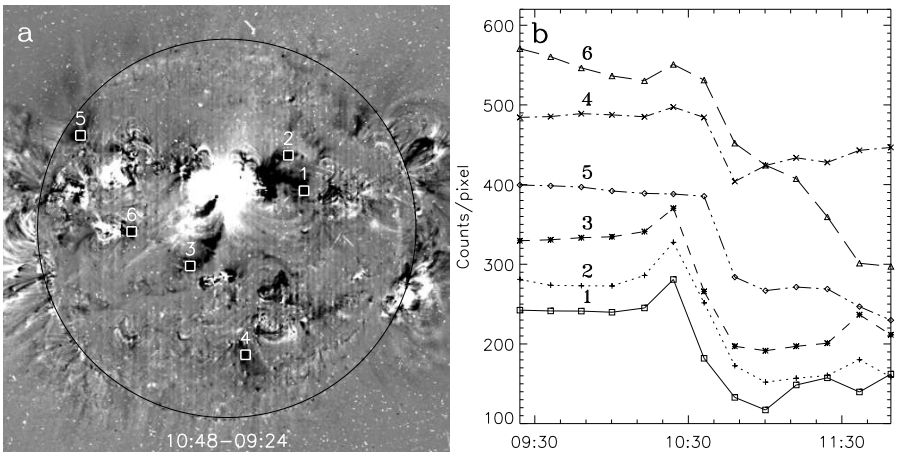

Figure 4. Several 10 × 10 pixel dimming areas in the 195 Å derotated difference image between 10:48 and 09:24 UT (a) and corresponding light curves of the average intensity inside them (b).

and configuration repeat the main south (1–2) and west (5–6) dimmings observed in the coronal lines 171 and 195 Å.

3.4. Evolution of the dimmings

Let us return to the 195 Å heliograms to study the evolution of the observed dimmings quantitatively. In particular, we take an interest in extent of the decrease of the EUV emission inside them (i.e. the depth of the dimmings) and its time variations. For that, we have selected several significant 10×10 pixel areas inside the main west and south dimmings, adjoining to the eruptive center, as well as inside three remote dimmings, as shown in Figure 4(a). At that, we tried to select such areas that were affected by the flare brightening and instrumental saturation in the least extent. Then we computed the light curves of average intensity in each area for the available heliograms at the time interval from 09:24 to 11:48 UT. To reduce the effects of the flare brightening at around 10:24 UT and the 'snowstorm' after 11:00 UT, the pixels inside the areas where the intensity exceeds 200 counts with respect to the preceding frame were excluded from calculations. The time profiles obtained in that way are shown in Figure 4(b).

The evolution of the main dimmings is very similar. In two branches (1, 2) of the west dimming and in the extremity (3) of the south dimming, the intensity keeps almost constant till 10:12 UT. Then, at 10:24 some increase takes place caused probably by the flare brightening. It is followed by a clear decrease that is continuing to 10:48–11:00 UT. The amplitude of this decrease relative to the pre-event level ranges

from 50 % for areas 1, 2 to 40 % for area 3. The subsequent intensity variations with a small increase at 11:36–11:48 UT appear to be due to a residual effect of the 'snowstorm'.

The south and northeast remote dimmings (areas 4, 5 and 6) display the analogous evolution. The differences in comparison with the main dimmings are that here the intensity decrease starts with a time delay of one 12-min interval (at 10:36 UT), and that their depth is somewhat less (20–40 %). These features point to a disturbance propagating from the eruptive center.

4. Discussion and Conclusions

Our analysis of the SOHO/EIT data demonstrates that the picture of the disturbances associated with the powerful flare and CME in the Bastille Day event of 14 July 2000, presented in Paper 1, is not correct. The reason is that it was based in fact on the consideration of the running-difference images displaying changes occurring during the 12-min intervals between two neighboring heliograms. Such a consideration brought the author of Paper 1 to the erroneous conclusion that the heated material, responsible for a large-area flare brightening, was ejected, and then a dimming was formed over roughly the same region covering the entire central region of the dick including the extended active region AR 9077 and its outskirts. It is quite obvious that this scenario contradicts to the well-known *Yohkoh*/SXT, SOHO/EIT and TRACE observations of the grandiose bright posteruptive arcade developing over the active region at this time (e.g., Aschwanden and Alexander, 2001; Masuda, Kosugi, and Hudson, 2001).

We have presented here a real picture of the disturbances using the EIT derotated fixed-difference images in the 195 Å line. These images were formed by the two-step procedure. First, to compensate the solar rotation, all heliograms were derotated to the time of the pre-event heliogram at 10:00 UT. Then this reference heliogram was subtracted from all subsequent derotated images. For the late heliograms starting from 11:00 UT, we also applied an additional technique of the suppression of the 'snowstorm' caused by energetic particles, coming to the SOHO spacecraft from this event.

Based on these images, we have shown that in the reality two main large dimmings were formed near the Bastille Day posteruptive arcade. One of the dimmings was transequatorial and extended southward along the west part of the pre-event loop system. Another dimming consisted of three branches, stretched westward, and occupied a large area between the eruptive center and a remote active region. Such dual

dimmings, joining to the posteruptive arcade, are usually believed to be footpoints of a magnetic flux rope structure that erupts as a CME (e.g., Thompson *et al.*, 1998; Zarro *et al.*, 1999; Sterling, 2000; Webb, 2000).

Besides these two dimmings, many other dimming structures, blobs and channels were scattered throughout the entire visible disk. This consists with a halo type of the observed CME and testifies to the global character of the CME and associated disturbances in this event.

In contrast to Paper 1, we have found some signatures of a coronal wave. As both the fixed and running-difference images display, an emitting front propagated from the eruptive center in the north direction through a large area that was free from any active regions. In the north polar region, this front slowed down, and its emission started to extend eastward, perhaps along the boundary of a polar coronal hole. Similar phenomena are observed in some other eruptive events with a large CME. One of such events was described by Thompson *et al.* (1998).

The techniques of the image derotation and the 'snowstorm' suppression has allowed us to form and to study specific difference images of the Bastille Day event from the 6-hour interval EIT heliograms at 171, 195, 284, and 304 Å. These images show that the main dimmings existed during at least several hours and that their location and configuration coincide completely or partly in the coronal lines 171, 195, 284 Å, as well as in the transition region line 304 Å. Such a multi-temperature analysis means that in this event the dimmings were mainly the results from the opening of the magnetic fields and evacuation of the matter during the CME eruption, and that not only coronal, but also transition-region plasma was involved in these processes, as it happened in other powerful CME events (see Chertok and Grechnev, 2003b,c).

The analysis of the quantitative characteristics of the 195 Å dimmings shows that in the main dimmings, adjoining to the eruptive center, the intensity decreases by a factor of about 2. This value is typical for other halo CME events (Zarro *et al.*, 1999; Chertok and Grechnev, 2003a,b). At the same time, in the remote dimmings, the drop of the intensity is observed somewhat latter, and its amplitude is about 20–40 %. These features mean that the remote structures are included in the CME process with some delay when the CME-initiated disturbance arrives at these regions.

Acknowledgements

We are grateful to the SOHO/EIT team members for data used in this research. SOHO is a mission of international cooperation between

ESA and NASA. We thank A.A. Golovko and O.I. Bugaenko for the discussions of the method. This work was supported by the Russian Foundation of Basic Research (grants 03-02-16049, 03-02-16591) and the Ministry of Industry and Science (grants 447.2003.2, 1445.2003.2).

References

Aschwanden, M. J. and Alexander, D.: 2001, *Solar Phys.*, **204**, 93.
Andrews, M. D.: 2001, *Solar Phys.*, **204**, 181 (Paper 1).
Brueckner, G. E, Howard, R. A., Koomen, M. J. *et al.*: 1995, *Solar Phys.*, **162**, 357.
Caroubalos, C, Alissandrakis, C. E., Hillaris, A. *et al.*: 2001, *Solar Phys.*, **204**, 165.
Chertok, I. M., Fomichev, V. V., Gnezdilov, A. A., Gorgutsa, R. V., Grechnev, V. V., Markeev, A. K., Nightingale, R. W., and Sobolev, D. E.: 2001, *Solar Phys.*, **204**, 141.
Chertok, I. M. and Grechnev, V. V.: 2003a, *Astron. Reports*, **47(2)**, 139.
Chertok, I. M. and Grechnev, V. V.: 2003b, *Astron. Reports*, **47(11)**, 934.
Chertok, I. M. and Grechnev, V. V.: 2003c, *Proc. ISCS 2003 Symposium, Tatranská Lomnica, Slovakia, 23-28 June 2003 (ESA SP-535, September 2003)*, p. 435.
Chertok, I. M., Grechnev, V. V., Hudson, H. S., and Nitta, N. V.: 2004a, *J. Geophys. Res.*, 109, A02112, doi:10.1029/2003JA010182.
Chertok, I. M., Slemzin, V. A., Kuzin, S. V., Grechnev, V. V., Bugaenko, O. I., Zhitnik, I. A., Ignatiev, A. P., and Pertsov, A. A.: 2004b, *Astron. Reports*, **81**, *in press.*
Delaboudinière, J.-P., Artzner, G. E., Brunaud, J. *et al.*: 1995, *Solar Phys.*, **162**, 291.
Deng, Y., Wang, J., Yan, Y., and Zhang, J.: 2001, *Solar Phys.*, **204**, 11.
Domingo, V., Fleck, B., and Poland, A. I.: 1995, *Solar Phys.*, **162**, 1.
Fletcher, L. and Hudson, H.: 2001, *Solar Phys.*, **204**, 71.
Gopalswamy, N. and Thompson, B. J.: 2000, *J. Atmos. Sol. Terr. Phys.* **62**, 1457.
Handy, B. N., Acton, L. W., Kankelborg, C. C. *et al.*: 1999, *Solar Phys.*, **187**, 229.
Hudson, H. S. and Cliver, E. W.: 2001, *J. Geophys. Res.*, **106**, 25199.
Karlický, M., Yan, Y., Fu, Q., Wang, S., Jiřička, K., Mészárosová, H., and Liu, Y.: 2001, *Astron. and Astrophys.*, **369**, 1104.
Klein, K.-L., Trottet, G., Lantos, P., and Delaboudinière, J.-P.: 2001, *Astron. Astrophys.*, **373**, 1073.
Kosovichev, A. G. and Zharkova, V. V.: 2001, *Astrophys. J.*, **550**, L105.
Livshits, M. A. and Belov, A. V.: 2004, *Astron. Reports*, *in press.*
Maia, D., Pick, M., Hawkins, S. E. III, Fomichev, V. V., and Jiřička, K.: 2001, *Solar Phys.*, **204**, 197.
Masuda, M., Kosugi, T., and Hudson, H. S.: 2001, *Solar Phys.*, **204**, 55.
Ogawara, Y., Takano, T., Kato, T. *et al.*: 1991, *Solar Phys.*, **136**, 1.
Oraevsky, V. N. and Sobelman, I. I.: 2002, *Astron. Lett.*, 28, 401.
Oraevsky, V. N., Sobelman, I. I., Zhitnik, I. A., Kuznetsov, V. D., Stepanov, A. I., Polishuk, G. M., Kovilin, P. N., Negoda, A. A., Dranovsky, V. I., and Yatskiv, Ya. S.: 2003, *Adv. Space Res.*, **32**, 2567.
Reiner, M. J., Kaiser, M. L., Karlický, M., Jiřička, K., and Bougeret, J.-L.: 2001, *Solar Phys.*, **204**, 121.
Share, G. H., Murphy, R. J., Tylka, A. J., Schwartz, R. A., Yoshimori, M., Suga, K., Nakayama, S., and Takeda, H.: 2001, *Solar Phys.*, **204**, 43.

Somov, B. V., Kosugi, T., Hudson, H. S., Sakao, T., and Masuda, S.: 2002, *Astrophys. J.*, **579**, 863.
Sterling, A. S.: 2000 *J. Atmosph. and Solar-Terr. Phys.* **62**, 1427.
Thompson, B. J., Plunkett, S. P., Gurman, J. B., Newmark, J. S., St.Cyr, O. C., and Michels, D. J.: 1998, *Geophys. Res. Lett.*, **25**, 2465.
Tian, L., Wang, J., Wu, D.: 2002, *Solar Phys.*, **209**, 375.
Webb, D. F.: 2000, *J. Atmosph. and Solar-Terr. Phys.*, **62**, 1415.
Yan, Y., Aschwanden, M. J., Wang, S., and Deng, Y.: 2001, *Solar Phys.*, **204**, 29.
Zarro, D. M., Sterling, A. S., Thompson, B. J., Hudson, H. S., and Nitta, N.: 1999, *Astrophys. J.*, **520**, L139.
Zhitnik, I. A., Bougaenko, O. I., Delaboudinière, J.-P. *et al.*: 2002, *Proc. 10th European Solar Physics Meeting, Prague (ESA SP-506)*, p. 915.